J Eng Math (2009) 64:237–250
DOI 10.1007/s10665-009-9278-y

Long-wavelength stability of an unsupported multilayer liquid film falling under gravity

R. J. Dyson · J. Brander · C. J. W. Breward · P. D. Howell

Received: 20 December 2006 / Accepted: 18 February 2009 / Published online: 8 March 2009

Abstract The long-wavelength stability of an unsupported multilayer liquid film falling under the effects of gravity and surface tension is investigated. By considering the Navier–Stokes equations for two fluid layers in the high-Reynolds-number and small-aspect-ratio limits the steady-state solutions are obtained. The stability criterion found by Lin (J Fluid Mech 104:111–118, 1981) for a one-layer fluid curtain is generalised to the two-layer case and the criterion for an n-layer curtain is established.

Keywords Asymptotics · Curtain coating · Mathematical modelling · Multilayer · Stability · Thin film

1 Introduction

1.1 Industrial curtain coating

Curtain coating is an industrial process [1], traditionally used to coat photographic materials, which is now being adopted by the paper industry [2]. Within curtain coating, a reservoir of coating mix, typically an aqueous suspension containing 20–70% solids and surfactants, is formed into a curtain of fluid using either a slot or a slide, as shown in Fig. 1. The curtain falls under gravity until it hits the substrate or "web" to be coated, which is conveyed quickly underneath. The coated substrate is passed through driers to evaporate off the water and thus the finished product is left with a solid coating.

R. J. Dyson · C. J. W. Breward · P. D. Howell
Mathematical Institute, University of Oxford, 24-29 St Giles', Oxford OX1 3LB, UK

R. J. Dyson (✉)
Centre for Plant Integrative Biology, University of Nottingham, Sutton Bonington LE12 5RD, UK
e-mail: rosemary.dyson@nottingham.ac.uk

C. J. W. Breward
e-mail: breward@maths.ox.ac.uk

P. D. Howell
e-mail: howell@maths.ox.ac.uk

J. Brander
ArjoWiggins, Butler's Court, Beaconsfield, Bucks HP9 IRT, UK

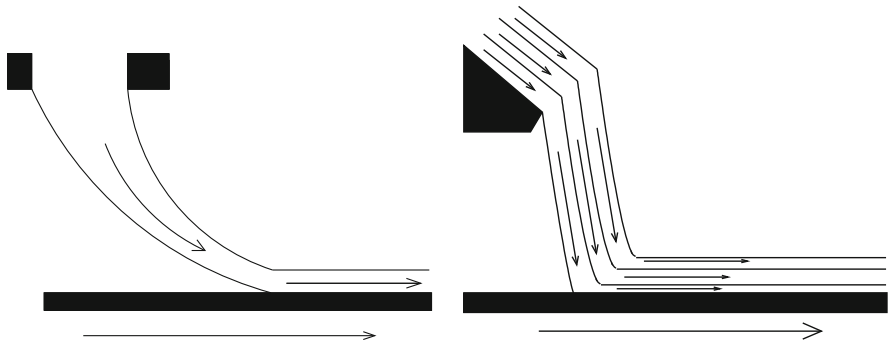

Fig. 1 A single-layer slot coater and a multi-layer slide coater

This technology is currently used, and well understood, within the photographic industry, and in the paper industry is starting to replace traditional methods of coating such as blade and air-knife coating [3]. In these methods, excess fluid is applied and the surplus scraped off, either mechanically or by means of air pressure, exerting a high shear stress on the substrate and risking frequent paper breaks. Use of curtain coating avoids these high shear stresses, but the operating conditions are far from those used in the photographic industry. In particular, the rheology of the liquids (especially the viscosity, which may be much lower for paper coating), the speed of the web (up to $1500\,\mathrm{m\,min^{-1}}$ as opposed to around $600\,\mathrm{m\,min^{-1}}$ in photographic coating) and the chemistry of the substrate are markedly different.

One of the major areas of experimental research in the field of curtain coating is multilayer coating [4]. A curtain with multiple fluid layers, each of different viscosity, density and surface tension, is formed using a slide as in Fig. 1 (right) and applied to the substrate as for the single-layer case. Thus, several active layers can be applied simultaneously, reducing the time taken to produce a finished product and hence the energy consumption for the driers. In the photographic industry successful curtains of upwards of 15 layers can be produced; however, these layers tend to comprise of mix with the same rheology but just different colour. In the paper industry, each layer in the coating is required to house different amounts of pigment and hence have different rheology.

1.2 Industrial issues with curtain coating

Problems affecting the coating quality arise in three distinct areas of the curtain: the sheet-forming zone (e.g. on the slide), the unsupported region as the curtain falls, and the impingement zone where the curtain meets the web [5]. In the sheet-forming zone, the "teapot effect" can be observed [6]. Within the unsupported region of the curtain, the ability to form and maintain a stable curtain is the major issue (see, for example, [7–9]). Finally, the majority of defects in the finished product originate in the impingement zone. Air entrainment occurs when the substrate is moving too fast, whereupon the fluid in the curtain does not wet the substrate properly [10]. This is due to the maximum speed of wetting of the dynamic contact line where the substrate, fluid and surrounding gas meet. As the speed of the substrate is increased, a thin layer of air is trapped and the contact line moves downstream before breaking into straight-line segments so that "sawteeth" appear. This causes air bubbles to be entrained between the coating and the substrate and therefore defects such as bubbles, pin holes and streaks appear [11]. There is a strong dependence of the web speed at the onset of air entrainment on the curtain flow rate; this is termed "hydrodynamic assist" [12]. A detailed discussion of recent developments on the physics of moving contact lines is given in [13].

1.3 Previous models and experimental studies

A general literature survey on coating methods is given in [3]. This includes work on more general aspects of coating, such as the flow of a thin film, the boundary layer formed along a moving wall in a semi-infinite fluid, as in

the Sakiadis model [14], and the dynamic wetting line, as well as areas more closely related to curtain coating such as the stability of the curtain [8], the propagation of waves in the fluid on the slide [15] and the flow in the curtain.

Experimental and theoretical stability analyses, as in [16] and [17], find a single-layer curtain to be stable if any disturbances in the curtain are "swept away" downstream before they have a chance to grow, *i.e.*, if the system has convective stability. This equates mathematically to a condition on the local Weber number, We, the ratio between inertia and surface tension forces:

$$\mathrm{We} = \frac{V\rho\tilde{q}}{2\gamma}. \tag{1}$$

Here ρ is the density, $\tilde{q}$ is the volumetric liquid flux, V is the local fluid speed and γ is the surface tension, assumed constant. By considering long-wavelength disturbances in a Newtonian fluid, neglecting any surfactant effects, Lin [17] obtained the local stability criterion

$$\mathrm{We} > 1, \tag{2}$$

which is widely used by industrial coating practitioners, in particular our industrial collaborators ArjoWiggins, who set their operating conditions to be consistent with (2). We note here that Lin's definition of the Weber number is the inverse of that traditionally used.

In his recent book [18, pp. 26–86], Lin discusses many of the different analyses and experiments which have been performed to shed light on the veracity of the Weber number condition (2). For example, incorporating the effects of the density of the air surrounding the curtain can induce convective instability and incorporating the viscosity of the curtain and/or the surrounding gas alters the critical Weber number at which the curtain loses convective stability, though only by a small amount. However, the essential details of the breakup process are captured by models that neglect these two effects.

It should be emphasised that (2) is a sufficient but not necessary condition for the curtain to be stable. Finnicum et al. [7] and Lin and Roberts [19] both find experimentally that the curtain is stable when the criterion (2) is satisfied, but that it may remain stable when the flow rate is reduced so that the criterion is violated. Finnicum et al. [7] state that extreme care was taken not to disturb the curtain, whilst Lin and Roberts [19] notice that the rim of the disturbance accumulates additional mass, and therefore the curtain thickness becomes large, violating the assumption that the curtain is thin. They conclude that this additional mass is important for stability calculations. This was confirmed by Roche et al. [20] who introduced a needle into a curtain to investigate the response of the curtain to local perturbations. They found that, once a stable curtain has been formed, the curtain may be maintained as We is reduced to approximately $\mathrm{We} = 0.7$ where the onset of oscillations occurs; the curtain rising from the needle, collecting additional mass into the rim which drives the free edge back to the needle where this additional mass is shed. Once the curtain breaks up, a significant increase in flux is required for it to reform.

Obviously, within an industrial setting there will always be disruptions which cannot be controlled and therefore a robust criterion is required. Hence, even with the restrictions on the validity (2), it is found to be useful by industrial coating practitioners. It ensures the curtain is robust to stability issues for the majority of its descent, and that it will spontaneously reform if it does rupture for any reason. We note, however, that it does not ensure stability in the impingement zone; it only ensures the formation of a stable curtain prior to impingement [11]; this is another serious issue within curtain coating which we do not address in this paper.

The paper-coating industry is particularly concerned with understanding the formation and maintenance of stable multilayer curtains, (they believe that the wetting line instability can be controlled by reducing paper-surface roughness and coating-mix surface tension, and ensuring that air entrainment baffles are properly in place). Mathematical models of multilayer flows, however, concentrate solely on the case where the film is on a substrate, for instance in [21]. These models can be applied to the flow on the slide, but not to the flow in the unsupported region of the curtain. We wish to investigate that region here, with a particular emphasis on stability. In this paper we establish a model for a two-layer falling film and investigate its stability. We then generalise our approach by considering an n-layer film.

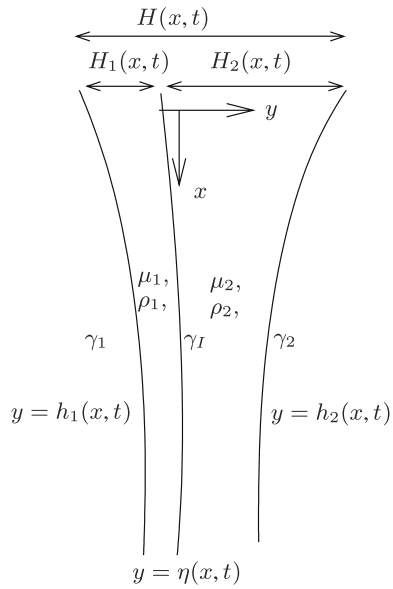

Fig. 2 A two-layer film falling under gravity

2 Two-fluid layer model

2.1 Assumptions

We first investigate the stability of a two-layer film falling under gravity; the two layers have different (but each constant) viscosities μ_1, μ_2 and densities ρ_1, ρ_2, as shown in Fig. 2. We neglect the effect of surfactants in this model and so also take constant surface tensions γ_1, γ_2 and constant interface tension γ_I. We take a cross-section through the centre of the curtain far away from any edge effects, so we only consider the problem in two dimensions.

We assume both fluids are Newtonian; this is clearly not physically accurate, since the fluids of interest contain 20–70% solids, but significantly simplifies our model. Lin [17] also makes this assumption to derive (2) which is widely used within industry. Therefore we expect to obtain industrially useful results, but we note that our current work involves generalising our models to non-Newtonian fluids.

We neglect the effect of the web on the curtain; a more accurate model of the curtain coating process including the boundary layer near the substrate may be found in [22]. We also assume that the fluid in the curtain has evolved to plug flow before we start the modelling process; the inner problem in which the curtain leaves the slot or the slide is not considered here. This problem has been studied for the one-fluid case in [23] and [24], for example.

We choose our coordinate system with x pointing vertically downwards such that $x = 0$ at the top of the curtain, and we take $y = 0$ at the initial centre of mass of the curtain cross-section.

2.2 Dimensional equations

It is helpful to consider the more general problem of a single fluid with variable density ρ and viscosity μ such that each convects with the flow, that is

$$\frac{\partial \rho}{\partial t} + (\mathbf{u} \cdot \nabla)\rho = 0, \tag{3}$$

$$\frac{\partial \mu}{\partial t} + (\mathbf{u} \cdot \nabla)\mu = 0. \tag{4}$$

We recover the situation of interest later by taking ρ and μ to be piecewise constant in each of the separate fluid layers. The flow is then governed by the compressible Navier–Stokes equations,

$$\rho\left(\frac{\partial \mathbf{u}}{\partial t}+(\mathbf{u}\cdot\nabla)\,\mathbf{u}\right)=\nabla\cdot\boldsymbol{\sigma}+\rho g\mathbf{i}, \tag{5}$$

$$\frac{\partial \rho}{\partial t}+\nabla\cdot(\rho\mathbf{u})=0, \tag{6}$$

where $\mathbf{u}=(u,v)$ is the velocity, $\boldsymbol{\sigma}$ is the stress tensor and $\mathbf{i}$ is the unit vector pointing in the direction of increasing x.

On the two air-liquid interfaces $y=h_1(x,t)$ and $y=h_2(x,t)$, we have the kinematic condition

$$\frac{\partial h_j}{\partial t}+u_j\frac{\partial h_j}{\partial x}=v_j \quad \text{on } y=h_j(x,t), \tag{7}$$

and, in addition, a force balance gives

$$\boldsymbol{\sigma}_j\cdot\mathbf{n}_j=-\gamma_j\left(\nabla\cdot\mathbf{n}_j\right)\,\mathbf{n}_j \quad \text{on } y=h_j(x,t), \tag{8}$$

where $\mathbf{n_j}$ is the outward-pointing normal to the surface.

When we take ρ and μ to be piecewise constant, with the discontinuity at $y=\eta(x,t)$, we also impose continuity of velocity and the kinematic condition, so that

$$u_1=u_2, \quad v_1=v_2 \quad \text{on } y=\eta(x,t), \tag{9}$$

$$\frac{\partial \eta}{\partial t}+u\frac{\partial \eta}{\partial x}=v \quad \text{on } y=\eta(x,t). \tag{10}$$

Finally, also on this fluid–fluid interface, a force balance gives

$$\left[\boldsymbol{\sigma}_j\cdot\mathbf{n}\right]_1^2=-\gamma_I\,(\nabla\cdot\mathbf{n})\,\mathbf{n} \quad \text{on } y=\eta(x,y). \tag{11}$$

Before nondimensionalising, it is helpful to derive exact integral relations from (5)–(8) representing net momentum balances in the longitudinal and transverse directions.

2.2.1 Net momentum balances

Using (6) and (3) we may rewrite the x-component of (5) as

$$\frac{\partial}{\partial t}(\rho u)+\frac{\partial}{\partial x}\left(\rho u^2\right)+\frac{\partial}{\partial y}(\rho uv)=\frac{\partial \sigma_{xx}}{\partial x}+\frac{\partial \sigma_{xy}}{\partial y}+\rho g. \tag{12}$$

Integrating this with respect to y across the thickness of the curtain, and using the first component of (8), we find

$$\begin{aligned}\frac{\partial}{\partial t}\int_{h_1}^{h_2}\rho u\,\mathrm{d}y+\frac{\partial}{\partial x}\int_{h_1}^{h_2}\rho u^2\,\mathrm{d}y=\int_{h_1}^{h_2}\rho g\,\mathrm{d}y+\frac{\partial}{\partial x}\int_{h_1}^{h_2}\sigma_{xx}\,\mathrm{d}y\\ -\frac{\gamma_1\dfrac{\partial^2 h_1}{\partial x^2}\dfrac{\partial h_1}{\partial x}}{\left(1+\left(\dfrac{\partial h_1}{\partial x}\right)^2\right)^{3/2}}-\frac{\gamma_I\dfrac{\partial^2 \eta}{\partial x^2}\dfrac{\partial \eta}{\partial x}}{\left(1+\left(\dfrac{\partial \eta}{\partial x}\right)^2\right)^{3/2}}-\frac{\gamma_2\dfrac{\partial^2 h_2}{\partial x^2}\dfrac{\partial h_2}{\partial x}}{\left(1+\left(\dfrac{\partial h_2}{\partial x}\right)^2\right)^{3/2}}.\end{aligned} \tag{13}$$

This represents a net momentum balance in the x-direction.

We next consider the transverse balance. Using (6) and (3) we may rewrite the y-component of (5) as

$$\frac{\partial}{\partial t}(\rho v)+\frac{\partial}{\partial x}(\rho uv)+\frac{\partial}{\partial y}\left(\rho v^2\right)=\frac{\partial \sigma_{xy}}{\partial x}+\frac{\partial \sigma_{yy}}{\partial y}. \tag{14}$$

Integrating with respect to y between h_1 and h_2, and using the first component of (8), we find

$$\frac{\partial}{\partial t}\int_{h_1}^{h_2}\rho v\,\mathrm{d}y+\frac{\partial}{\partial x}\int_{h_1}^{h_2}\rho uv\,\mathrm{d}y=\frac{\partial}{\partial x}\int_{h_1}^{h_2}\sigma_{xy}\,\mathrm{d}y$$
$$+\frac{\gamma_1\dfrac{\partial^2 h_1}{\partial x^2}}{\left(1+\left(\dfrac{\partial h_1}{\partial x}\right)^2\right)^{3/2}}+\frac{\gamma_I\dfrac{\partial^2\eta}{\partial x^2}}{\left(1+\left(\dfrac{\partial\eta}{\partial x}\right)^2\right)^{3/2}}+\frac{\gamma_2\dfrac{\partial^2 h_2}{\partial x^2}}{\left(1+\left(\dfrac{\partial h_2}{\partial x}\right)^2\right)^{3/2}}. \tag{15}$$

This represents a net momentum balance in the y-direction.

2.3 Nondimensionalisation

We now nondimensionalise using

$$u_j=U\hat{u}_j,\quad v_j=\delta U\hat{v}_j,\quad x=l\hat{x},\quad y=\delta l\hat{y},\quad t=\frac{l}{U}\hat{t},\quad \sigma_j=\frac{\mu_1 U}{l}\hat{\sigma}_j,\quad p_j=\frac{\mu_1 U}{l}\hat{p}_j, \tag{16}$$

where U is a typical velocity in the curtain as it exits the slot, l is a typical length of the curtain (e.g. the height of the coater above the substrate), h_0 is the initial thickness of the curtain and $\delta=h_0/l$ is the aspect ratio. We take $\delta\ll 1$, and so are looking for long-wavelength behaviour; this is the same limit as in [17].

Nondimensionalising (5) and (6), immediately dropping hats for clarity, allowing ρ and μ to be piecewise constant such that

$$\rho=\begin{cases}1 & h_1\le y<\eta\\ \rho_2/\rho_1 & \eta<y\le h_2,\end{cases} \tag{17}$$

$$\mu=\begin{cases}1 & h_1\le y<\eta\\ \mu_2/\mu_1 & \eta<y\le h_2,\end{cases} \tag{18}$$

and assuming we have a Newtonian fluid so that

$$\sigma_{jxx}=-p_j+2\frac{\mu_j}{\mu_1}\frac{\partial u_j}{\partial x}, \tag{19}$$

$$\sigma_{jxy}=\frac{\mu_j}{\mu_1}\left(\frac{1}{\delta}\frac{\partial u_j}{\partial y}+\delta\frac{\partial v_j}{\partial x}\right), \tag{20}$$

$$\sigma_{jyy}=-p_j+2\frac{\mu_j}{\mu_1}\frac{\partial v_j}{\partial y}, \tag{21}$$

we find

$$\delta^2\mathrm{Re}\left(\frac{\partial u_1}{\partial t}+u_1\frac{\partial u_1}{\partial x}+v_1\frac{\partial u_1}{\partial y}\right)=\frac{\partial^2 u_1}{\partial y^2}+\delta^2\left(\frac{\partial^2 u_1}{\partial x^2}+\frac{\mathrm{Re}}{\mathrm{Fr}^2}-\frac{\partial p_1}{\partial x}\right), \tag{22}$$

$$\delta^2\mathrm{Re}\left(\frac{\partial v_1}{\partial t}+u_1\frac{\partial v_1}{\partial x}+v_1\frac{\partial v_1}{\partial y}\right)=-\frac{\partial p_1}{\partial y}+\delta^2\frac{\partial^2 v_1}{\partial x^2}+\frac{\partial^2 v_1}{\partial y^2}, \tag{23}$$

$$\begin{aligned}&\frac{\delta^2\mathrm{Re}\,\rho_2}{\rho_1}\left(\frac{\partial u_2}{\partial t}+u_2\frac{\partial u_2}{\partial x}+v_2\frac{\partial u_2}{\partial y}\right)=\frac{\mu_2}{\mu_1}\frac{\partial^2 u_2}{\partial y^2}+\delta^2\left(\frac{\mu_2}{\mu_1}\frac{\partial^2 u_2}{\partial x^2}+\frac{\rho_2\mathrm{Re}}{\rho_1\mathrm{Fr}^2}-\frac{\partial p_2}{\partial x}\right),\\ &\frac{\delta^2\mathrm{Re}\,\rho_2}{\rho_1}\left(\frac{\partial v_2}{\partial t}+u_2\frac{\partial v_2}{\partial x}+v_2\frac{\partial v_2}{\partial y}\right)=-\frac{\partial p_2}{\partial y}+\frac{\mu_2}{\mu_1}\left(\frac{\partial^2 v_2}{\partial y^2}+\delta^2\frac{\partial^2 v_2}{\partial x^2}\right),\end{aligned} \tag{24}$$

$$\frac{\partial u_j}{\partial x}+\frac{\partial v_j}{\partial y}=0. \tag{25}$$

Here $\mathrm{Re} = \rho_1 U l/\mu_1$ is the Reynolds number based on the material properties of fluid 1 and $\mathrm{Fr} = U/\sqrt{gl}$ is the Froude number.

Finally, nondimensionalising the boundary conditions we find

$$\frac{\partial h_j}{\partial t} + u_j \frac{\partial h_j}{\partial x} = v_j \quad \text{on } y = h_j(x,t), \tag{26}$$

$$\frac{\partial \eta}{\partial t} + u \frac{\partial \eta}{\partial x} = v \quad \text{on } y = \eta(x,t), \tag{27}$$

$$u_1 = u_2, \quad v_1 = v_2 \quad \text{on } y = \eta(x,y), \tag{28}$$

$$\boldsymbol{\sigma}_j \cdot \mathbf{n}_j = (-1)^j \frac{\delta \gamma_j}{\mathrm{Ca}\gamma_1} \frac{\dfrac{\partial^2 h_j}{\partial x^2}}{\left(1 + \delta^2 \left(\dfrac{\partial h_j}{\partial x}\right)^2\right)^{3/2}} \mathbf{n}_j, \tag{29}$$

on $y = h_j(x,y)$.

$$\left[\boldsymbol{\sigma}_j \cdot \mathbf{n}\right]_{j=1}^{2} = \frac{\delta \gamma_I}{\mathrm{Ca}\gamma_1} \frac{\dfrac{\partial^2 \eta}{\partial x^2}}{\left(1 + \delta^2 \left(\dfrac{\partial \eta}{\partial x}\right)^2\right)^{3/2}} \mathbf{n}, \tag{30}$$

on $y = \eta(x,t)$, where

$$\mathbf{n}_j = (-1)^j \left[1 + \delta^2 \left(\frac{\partial h_j}{\partial x}\right)^2\right]^{-1/2} \begin{pmatrix} \delta \dfrac{\partial h_j}{\partial x} \\ -\left(1 + \delta^2 \left(\dfrac{\partial h_j}{\partial x}\right)^2\right)^{1/2} \end{pmatrix}, \tag{31}$$

$$\mathbf{n} = \left[1 + \delta^2 \left(\frac{\partial \eta}{\partial x}\right)^2\right]^{-1/2} \begin{pmatrix} -\delta \dfrac{\partial \eta}{\partial x} \\ \left(1 + \delta^2 \left(\dfrac{\partial \eta}{\partial x}\right)^2\right)^{1/2} \end{pmatrix}, \tag{32}$$

and $\mathrm{Ca} = \mu_1 U/\gamma_1$ is the Capillary number. Throughout we have based our nondimensionalisation on fluid 1 without loss of generality.

2.4 Asymptotic analysis

By taking typical values from the paper industry as in Table 1 we find

$$\delta \approx 10^{-3}, \quad \mathrm{Re} \approx 10^3, \quad \mathrm{Fr} \approx 1, \quad \mathrm{Ca} \approx 10, \tag{33}$$

and so we take the limit $\delta \to 0, \delta\,\mathrm{Re} = \mathcal{R} = O(1), \mathrm{Ca} = O(1), \mathrm{Fr} = O(1)$. The figures in Table 1 also suggest that we operate in the regime where μ_2/μ_1, ρ_2/ρ_1, γ_2/γ_1, γ_I/γ_1 are all $O(1)$.

Table 1 Approximate values for a two-layer curtain in the paper industry (provided by ArjoWiggins)

Quantity	Fluid 1	Fluid 2	Quantity
ρ	$1.6 \times 10^3\,\mathrm{kg\,m^{-3}}$	$1.006 \times 10^3\,\mathrm{kg\,m^{-3}}$	$h_0 = 10^{-4}\,\mathrm{m}$
$\tilde{q}$	$10^{-4}\,\mathrm{m^3\,s^{-1}}$	$0.75 \times 10^{-4}\,\mathrm{m^3\,s^{-1}}$	$l = 10^{-1}\,\mathrm{m}$
γ	$3 \times 10^{-2}\,\mathrm{N\,m^{-2}}$	$4 \times 10^{-2}\,\mathrm{N\,m^{-2}}$	$\gamma_I = 10^{-3}\,\mathrm{N\,m^{-2}}$
μ	$10^{-1}\,\mathrm{kg\,m^{-1}\,s^{-1}}$	$10^{-1}\,\mathrm{kg\,m^{-1}\,s^{-1}}$	$U = 0.7\,\mathrm{m\,s^{-1}}$

2.4.1 Leading-order solution

We solve (22)–(25), subject to (26)–(30), letting $\delta \to 0$ while $\mathcal{R} = O(1)$, and find

$$u_1 = u_2 = u(x,t),\ v_1 = v_2 = -\frac{\partial u}{\partial x} y + c(x,t), \tag{34}$$

$$p_1 = -2\frac{\partial u}{\partial x},\ p_2 = -2\frac{\mu_2}{\mu_1}\frac{\partial u}{\partial x}, \tag{35}$$

$$c(x,t) = \frac{\partial h_j}{\partial t} + \frac{\partial}{\partial x}\left(u h_j\right) = \frac{\partial \eta}{\partial t} + \frac{\partial}{\partial x}\left(u\eta\right). \tag{36}$$

Since we have three expressions for $c(x,t)$, by suitable pairwise subtraction we obtain the evolution equations

$$\frac{\partial H_j}{\partial t} + \frac{\partial}{\partial x}\left(u H_j\right) = 0, \tag{37}$$

for the two layer thicknesses $H_1 = \eta - h_1$, $H_2 = h_2 - \eta$, with $H_1 + H_2 = H$.

Note here that we have plug flow, that is, the velocity down the curtain is a function of x and t only, not of y. The system (34)–(35) is a two-fluid extension, including surface tension, to the Trouton model [25] for extensional flow; as in that model, we must consider the next terms in our expansion in order to close the leading-order model and hence complete our solution. The global force balances (13) and (15) provide a short cut to the derivation of these second-order terms.

2.4.2 Second-order solution

We determine our longitudinal equation at second order by inserting our first-order solution (34)–(35) in the dimensionless version of (13), letting $\delta \to 0$ and evaluating the integrals, the resulting equation is

$$\frac{\partial u}{\partial t} + u\frac{\partial u}{\partial x} - \frac{1}{\mathrm{Fr}^2} = 0. \tag{38}$$

To find the transverse equation we similarly substitute (34)–(35) in the dimensionless version of (15) and evaluate the integrals. It transpires that it is easier to work in terms of variables u, H_1, H_2, and the cross-sectional centre of mass $\bar{y}$ defined by

$$\int_{h_1}^{h_2} \rho y \,\mathrm{d}y = \bar{\rho} H \bar{y} = \frac{\left(\eta^2 - h_1^2\right)}{2} + \frac{\rho_2\left(h_2^2 - \eta^2\right)}{2\rho_1}, \tag{39}$$

where the mean density $\bar{\rho}$ is defined such that

$$\int_{h_1}^{h_2} \rho \,\mathrm{d}y = \bar{\rho} H, \tag{40}$$

so that

$$\bar{y} = \eta + \frac{\rho_2 H_2^2 - \rho_1 H_1^2}{2\left(\rho_1 H_1 + \rho_2 H_2\right)}. \tag{41}$$

Hence, again letting $\delta \to 0$ in (15), we find

$$\mathcal{R}\left(H_1 + \frac{\rho_2}{\rho_1} H_2\right)\frac{\mathrm{D}^2\bar{y}}{\mathrm{D}t^2} = \frac{1}{\mathrm{Ca}}\left(\frac{\gamma_2}{\gamma_1}\frac{\partial^2 h_2}{\partial x^2} + \frac{\partial^2 h_1}{\partial x^2} + \frac{\gamma_I}{\gamma_1}\frac{\partial^2 \eta}{\partial x^2}\right), \tag{42}$$

where $\mathrm{D}/\mathrm{D}t = \partial/\partial t + u\ \partial/\partial x$ is the leading-order convective derivative. This equation is a balance between the transverse momentum and the restoring force due to surface tension. In the parameter regime of interest, viscous

effects are found to be negligible in the majority of the curtain. Note that, for ease of presentation, we have not yet substituted for h_j and η in terms of H_j and $\bar{y}$ into the right-hand side of (42).

We now have four equations, (37), (38) and (42), for our four unknowns $u(x,t)$, $H_1(x,t)$, $H_2(x,t)$ and $\bar{y}(x,t)$. To proceed we must impose boundary conditions. We nondimensionalise such that $u = 1$ at $x = 0$ and prescribe the respective nondimensional fluxes q_1, q_2 of each fluid. As mentioned earlier, we take the origin of our coordinate system to be the point where the centroid exits the slot, *i.e.* $\bar{y} = 0$ at $x = 0$ and we must also prescribe the angle at which the curtain exits the slot. For simplicity we assume that the centroid $\bar{y}$ exits vertically, but we note that in practice multilayer curtains tend to flow from slides, which would produce a non-zero initial angle. We expect this to give a good "outer" solution though, and since we are interested in the stability of the curtain this should suffice.

Hence we impose the initial conditions

$$u = 1, \quad uH_j = q_j, \quad \bar{y} = \frac{\partial \bar{y}}{\partial x} = 0 \quad \text{at} \quad x = 0. \tag{43}$$

2.5 Leading-order solutions

2.5.1 Steady state

We look for a steady-state solution, and find

$$u = \sqrt{2x/\mathrm{Fr}^2 + 1}, \tag{44}$$

$$uH_j = q_j, \tag{45}$$

from (37) and (38). Substituting these solutions in (42) and differentiating as appropriate, we find we are left to solve

$$\left(u^2 - \Gamma u\right)\frac{\partial^2 \bar{y}}{\partial x^2} + \frac{1}{\mathrm{Fr}^2}\frac{\partial \bar{y}}{\partial x} = \frac{C}{\left(2x/\mathrm{Fr}^2 + 1\right)^2}, \tag{46}$$

for $\bar{y}$, where

$$\Gamma = \frac{\gamma_1 + \gamma_2 + \gamma_I}{\mathrm{Ca}\ \gamma_1\ \mathcal{R}\left(q_1 + \dfrac{\rho_2}{\rho_1}q_2\right)} \tag{47}$$

is a ratio between surface tension and inertia forces, equivalent to an inverse Weber number, and

$$C = \frac{3\left(\dfrac{\gamma_2}{\gamma_1}q_2 - q_1 + \left(1 + \dfrac{\gamma_I}{\gamma_1} + \dfrac{\gamma_2}{\gamma_1}\right)\dfrac{q_1^2 - \dfrac{\rho_2}{\rho_1}q_2^2}{2\left(q_1 + \dfrac{\rho_2}{\rho_1}q_2\right)}\right)}{\mathrm{Fr}^4\ \mathrm{Ca}\ \mathcal{R}\left(q_1 + \dfrac{\rho_2}{\rho_1}q_2\right)} \tag{48}$$

is the constant found upon grouping together the forcing terms on the right-hand side of (46).

To solve we transform the independent variable to $\zeta = 2x/\mathrm{Fr}^2 + 1$ and find

$$2(\zeta - \Gamma\sqrt{\zeta})\frac{\partial^2 \bar{y}}{\partial \zeta^2} + \frac{\partial \bar{y}}{\partial \zeta} = \frac{\mathrm{Fr}^4 C}{2\zeta^2}, \tag{49}$$

with $\bar{y} = \partial\bar{y}/\partial\zeta = 0$ at $\zeta = 1$, which yields

$$\bar{y} = \frac{C\mathrm{Fr}^4}{3}\left(\sqrt{\zeta} - 1 + \frac{1}{\Gamma}\left(1 - \frac{1}{\sqrt{\zeta}}\right) + \frac{1}{2\Gamma^2}\log\zeta + \left(\Gamma - \frac{1}{\Gamma^2}\right)\left(\log\left(\sqrt{\zeta} - \Gamma\right) - \log\left(1 - \Gamma\right)\right)\right). \tag{50}$$

Since we have neglected the web, we have no directionality for coating; coating AB (where AB represents fluid A as fluid 1 and fluid B as fluid 2) or BA gives two curtains which are merely reflections of each other. Initially the curtain will bend towards $y > 0$ if $\partial^2 \bar{y}/\partial x^2 > 0$, that is if

$$\frac{C}{1-\Gamma} > 0. \tag{51}$$

Assuming the coater is located in $y < 0$, this gives a criterion for the curtain to bend away from the coater, thus reducing the risk of the "teapot" effect [6]. In addition, there will be directionality in the system if the curtain is leaving a slide rather than a slot because this will impart a non-zero initial gradient. In this case, swapping AB for BA could give very different curtain shapes.

We also note that if we neglect surface tension (i.e., let $\mathrm{Ca} \to \infty$) we have $C = 0$ and so $\bar{y} = 0$; this is to be expected, since $\bar{y}$ represents the centroid of the curtain. Similarly, taking identical values of density, surface tension and flux for both fluids we again have $C = 0$, and so $\bar{y} = 0$; in this case $\bar{y}$ represents the centreline of a single fluid curtain.

2.5.2 Typical dimensional steady states

We first note that (44) is the free-fall velocity as found by Brown [16] for the one-fluid case; similarly the expression (45) for H_j is analogous to the total thickness of a curtain of one fluid [22].

We plot typical dimensional steady states in Figs. 3–6. We first show a typical curtain using realistic values and then take greatly differing values of the various constants to demonstrate the effect they have. Note that, whilst the latter three do not represent physically realistic coating scenarios, this is a useful exercise to isolate the effects of altering each of the three properties (density, flux and surface tension) that vary across the layers in turn. We take as

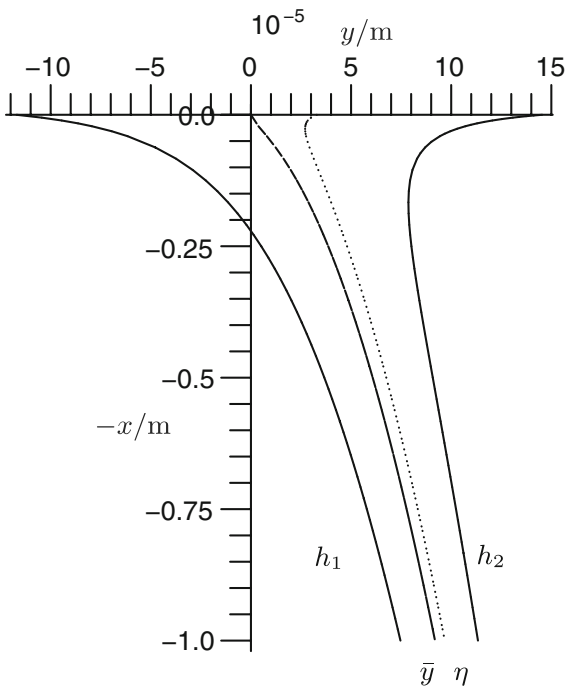

Fig. 3 A dimensional steady state with typical industrial values, taking $\rho_1 = 1.6 \times 10^3\,\mathrm{kg\,m^{-3}}$, $\rho_2 = 1.006 \times 10^3\,\mathrm{kg\,m^{-3}}$, $\tilde{q}_1 = 10^{-4}\,\mathrm{m^3\,s^{-1}}$, $\tilde{q}_2 = 0.75 \times 10^{-4}\,\mathrm{m^3\,s}$, $\gamma_1 = 3 \times 10^{-2}\,\mathrm{N\,m^{-2}}$ and $\gamma_2 = 4 \times 10^{-2}\,\mathrm{N\,m^{-2}}$. Here η gives the interface of the two fluids and $\bar{y}$ gives the position of the centroid

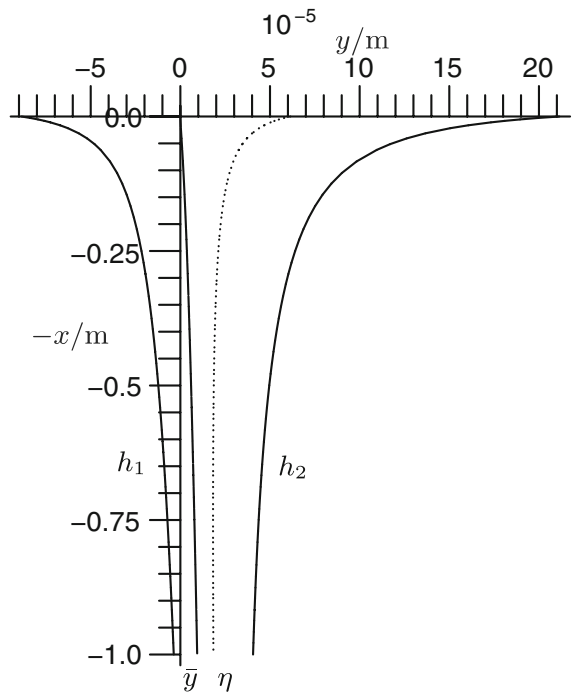

Fig. 4 A dimensional steady state with differing density, taking $\rho_1 = 10^4\,\mathrm{kg\,m^{-3}}$, $\rho_2 = 10^3\,\mathrm{kg\,m^{-3}}$. Here η gives the interface of the two fluids and $\bar{y}$ gives the position of the centroid

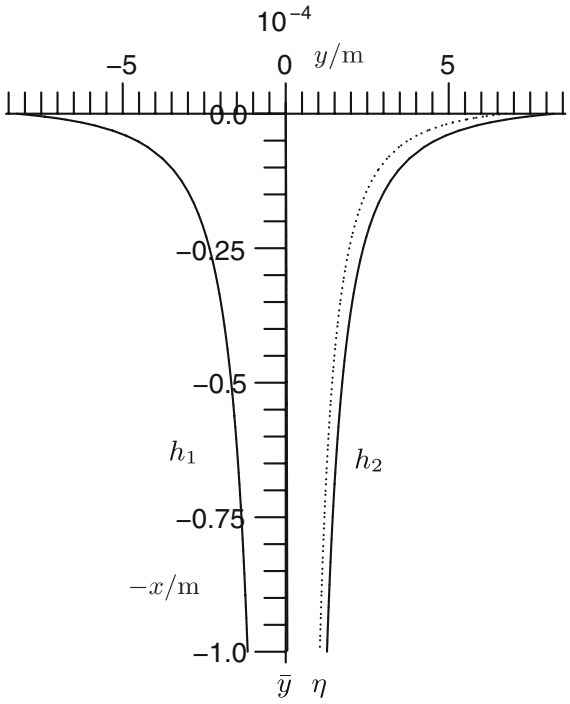

Fig. 5 A dimensional steady state with differing flux, taking $\tilde{q}_1 = 10^{-3}\,\mathrm{m^3\,s^{-1}}$ and $\tilde{q}_2 = 10^{-4}\,\mathrm{m^3\,s^{-1}}$. Here η gives the interface of the two fluids and $\bar{y}$ gives the position of the centroid

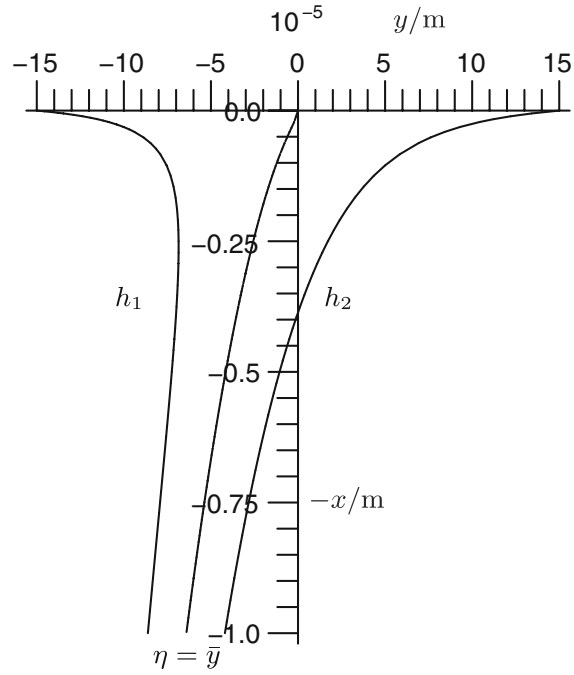

Fig. 6 A dimensional steady state with differing surface tension, taking $\gamma_1 = 2 \times 10^{-2}\,\mathrm{N\,m^{-2}}$ and $\gamma_2 = 10^{-2}\,\mathrm{N\,m^{-2}}$. Here η gives the interface of the two fluids and $\bar{y}$ gives the position of the centroid

standard values $\rho_j = 10^3\,\mathrm{kg\,m^{-3}}$, $\tilde{q}_j = 10^{-4}\,\mathrm{m^3\,s^{-1}}$, $U = 2/3\,\mathrm{m\,s^{-1}}$, $\gamma_j = 10^{-2}\,\mathrm{N\,m^{-2}}$ and $\gamma_I = 10^{-3}\,\mathrm{N\,m^{-2}}$; the captions to the figures only give the values we have changed.

In Fig. 3 we take typical industrial values as given in Table 1, with each value differing only slightly over the two layers. We see that the curtain is very slightly deflected to the right due to the difference in rheology.

In Fig. 4 we alter the density, taking $\rho_1 = 10^4\,\mathrm{kg\,m^{-3}}$, $\rho_2 = 10^3\,\mathrm{kg\,m^{-3}}$ and all other values the same across the two layers. This shows that layer 1 dominates, since it has more mass, and "pulls" layer 2 back towards it.

In Fig. 5 we change the fluxes, so that $\tilde{q}_1 = 10^{-3}\,\mathrm{m^3\,s^{-1}}$, $\tilde{q}_2 = 10^{-4}\,\mathrm{m^3\,s^{-1}}$, and find that layer 1 dominates; the profile given is very close to what we would expect if layer 2 were not present.

In Fig. 6, we alter the surface tensions so that $\gamma_1 = 2 \times 10^{-2}\,\mathrm{N\,m^{-2}}$, $\gamma_2 = 10^{-2}\,\mathrm{N\,m^{-2}}$. Note that $\bar{y} = \eta$, since momentum flux in both layers is equal. The much higher value of surface tension in layer 1 pulls the curtain to the left.

2.5.3 Convective stability

We obtain a homogeneous version of (42) by subtracting off the steady state, that is

$$\frac{\partial^2 \bar{y}^{(1)}}{\partial t^2} + 2u(x)\frac{\partial^2 \bar{y}^{(1)}}{\partial x \partial t} + \left(u^2(x) - \Gamma u(x)\right)\frac{\partial^2 \bar{y}^{(1)}}{\partial x^2} + \frac{1}{\mathrm{Fr}^2}\frac{\partial \bar{y}^{(1)}}{\partial x} = 0, \tag{52}$$

where $\bar{y}^{(1)} = \bar{y} - \bar{y}^{(0)}\,(x)$ and $y^{(0)}(x)$ is the steady state given by (50). We calculate the characteristics of (52) and find that they satisfy

$$\frac{\mathrm{d}x}{\mathrm{d}t} = u \pm \sqrt{u\Gamma}. \tag{53}$$

We now consider the sign of these characteristics with a view to determining the stability of the curtain. If both characteristics are positive, then information propagates downstream only, and so any disturbances will be swept away (*i.e.,* we will have convective stability). If, however, one of the characteristics is negative, disturbances and information from the impingement point may propagate upstream and so disrupt coating.

Only the characteristic given by $\mathrm{d}x/\mathrm{d}t = u - \sqrt{u\Gamma}$ has the possibility of disrupting the flow, and is negative only if $u < \sqrt{u\Gamma}$. Hence the condition for local convective stability of a two-fluid layer is

$$\frac{V\,(\rho_1\tilde{q}_1 + \rho_2\tilde{q}_2)}{\gamma_1 + \gamma_2 + \gamma_I} > 1, \tag{54}$$

where V is the local dimensional velocity. This is clearly a generalisation of the original one-fluid stability criterion which was given in (2).

This condition may be used to determine whether, given values for density, flux, surface tension and velocity, a stable curtain may be formed. If (54) is violated, it may be used to determine which modifications could be made to the fluids to enable coating to take place; for example how much we must reduce the surface tension to satisfy the criterion. This could be achieved for example by the addition of surfactant (although this may alter the force balances).

3 Generalisation to an *n*-fluid layer

We now generalise (54) to a condition for coating with n fluid layers, taking the jth-layer to have thickness H_j with surface/interface tension γ_j on the right-hand interface (so that we have tensions γ_0 to γ_n); the other notation generalises similarly. Thus, we may recast the leading-order governing equations as

$$\frac{\partial H_j}{\partial t} + \frac{\partial}{\partial x}\left(uH_j\right) = 0, \tag{55}$$

$$\frac{\partial u}{\partial t} + u\frac{\partial u}{\partial x} - \frac{1}{\mathrm{Fr}^2} = 0, \tag{56}$$

and, generalising our definition of $\bar{y}$,

$$\mathcal{R}\bar{\rho}H\frac{\mathrm{D}^2\bar{y}}{\mathrm{D}t^2} = \frac{1}{\mathrm{Ca}}\sum_{i=0}^{n}\frac{\gamma_i}{\gamma_0}\frac{\partial^2\bar{y}}{\partial x^2} + f(H_j), \tag{57}$$

where $f(H_j)$ is a known, but rather messy, function. Since this only alters the steady states but not their stability, we do not discuss it further.

In the steady state, the velocity $u(x)$ and thicknesses $H_j(x)$ are again given by (44) and (45). Furthermore, upon substituting H_j from (45) in (57), the resulting equation for $\bar{y}$ is the same as (46), with Γ given by

$$\Gamma = \frac{1}{\mathrm{Ca}}\frac{\sum_{i=0}^{n}\gamma_i/\gamma_0}{\mathcal{R}\sum_{i=1}^{n}\rho_i q_i/\rho_1}, \tag{58}$$

and where C has been appropriately modified; "n-layeredness" may thus merely be expressed inside the constants and the solution for $\bar{y}$ is given by (50) as before. We see the rest of the analysis from Sect. 2.5.3 will follow through exactly for the n-layer case and so the curtain will be stable provided $u > \sqrt{u\Gamma}$. Redimensionalising and taking u to be the local dimensional velocity V we have

$$\frac{V\sum_{j=1}^{n}\rho_j\tilde{q}_j}{\sum_{j=0}^{n}\gamma_j} > 1, \tag{59}$$

which generalises the Lin condition to n fluid layers. This condition may be used in a similar way as that for two fluid layers to ensure a viable curtain.

4 Conclusions and further work

Motivated by the industrial process of curtain coating, we have investigated the behaviour of an unsupported two-layer thin liquid sheet falling under gravity. By considering the Navier–Stokes equations in the high-Reynolds-number and small-aspect-ratio limits, we have derived the leading-order system of equations given by (37), (38) and (42), governing the evolution of the average velocity, layer thicknesses and centroid. Using steady-state solutions, we demonstrated the effects of varying density, flux and surface tension across the two layers, as shown in Sect. 2.5.1. By considering the characteristics of the flow we found a curtain to be convectively stable provided (54) is satisfied. We have also shown this criterion to be easily generalisable to (59) for an n-layer curtain. Both of these are clearly generalisations of the Lin stability criterion (2), which is widely used throughout industry to ensure stability during practical applications of curtain coating. For example, if a given process requires a certain flux, and the fluid being used has a certain density and surface tension, this criterion gives the minimum value of the local velocity to form a stable curtain. This criterion is now being used by ArjoWiggins to determine whether test mixes should run on their coater.

We note, however, that this work is only valid in the long-wavelength approximation; it remains to be determined whether our criterion (59) applies to short-wavelength disturbances. Similarly, we have considered only a Newtonian fluid, whereas the fluids used in actual coating procedures contain 20–70% solids and so this assumption is clearly invalid. This work should therefore be repeated for different rheologies to find a more widely applicable result. In addition we have taken constant surface tension when in fact the fluids contain surfactants, which gives another assumption that should be relaxed. All these assumptions were also used by Lin to find the original one-fluid condition, and therefore we expect this new condition to be industrially useful even with these restrictions.

Acknowledgements RJD gratefully acknowledges funding from the EPSRC and ArjoWiggins via a Smith Institute Industrial CASE award.

References

1. Mendez B, Morita H (2001) Curtain coating—a novel coating technique for high-precision coating. Wochenbl Papierfabr 129(22): 1492–1497
2. Trefz M (2005) Production experience with curtain coating for woodfree coated paper. TAPPI J 4(11):3–7
3. Weinstein S, Ruschak K (2004) Coating flows. Ann Rev Fluid Mech 36:29–53
4. Schweizer P (2002) Simultaneous multilayer coating technologies: attractiveness and limitations. In: Coating and graphic arts conference and trade fair. Tappi Press, Atlanta
5. Triantafillopoulos N, Gron J, Luostarinen I, Paloviita P (2004) Operational issues in high-speed curtain coating of paper, Part 1: the principles of curtain coating. TAPPI J 3(11):6–10
6. Kistler S, Scriven L (1994) The teapot effect: sheet forming flows with deflection wetting and hysteresis. J Fluid Mech 263:19–62
7. Finnicum D, Weinstein S, Ruschak K (1993) The effect of applied pressure on the shape of a two dimensional liquid curtain falling under the influence of gravity. J Fluid Mech 255:647–665
8. Pritchard W (1986) Instability and chaotic behaviour in a free-surface flow. J Fluid Mech 165:1–60
9. Triantafillopoulos N, Gron J, Luostarinen I, Paloviita P (2004) Operational issues in high-speed curtain coating of paper, Part 2: curtain coating of lightweight coated paper. TAPPI J 3(12):11–16
10. Blake T, Ruschak K (1979) A maximum speed of wetting. Nature 282:489–491
11. Blake T, Clarke A, Ruschak K (1994) Hydodynamic assist of dynamic wetting. AIChE 40:229–242
12. Marston J, Simmons M, Decent S, Kirk S (2006) Influence of the flow field in curtain coating onto a prewet substrate. Phys Fluids 18(112102)
13. Blake T (2006) The physics of moving contact lines. J Colloid Interface Sci 299:1–13
14. Sakiadis B (1961) Boundary layer behaviour on continuous solid surfaces. AIChE 7:26–28, 221–225, 467–470
15. Yih C (1963) Stability of liquid flow down an inclined plane. Phys Fluids 6:321–334
16. Brown D (1960) A study of the behaviour of a thin sheet of moving liquid. J Fluid Mech 10:297–305
17. Lin S (1981) Stability of a viscous liquid curtain. J Fluid Mech 104:111–118
18. Lin S (2003) Breakup of liquid sheets and jets. Cambridge University Press, Cambridge
19. Lin S, Roberts G (1981) Waves in a viscous liquid curtain. J Fluid Mech 114:443–458
20. Roche J, Grand NL, Brunet P, Lebon L, Limat L (2006) Perturbations on a liquid curtain near break-up: waves and free edges. Phys Fluids 18(082101)

21. Chen K (1993) Wave formation in the gravity-driven low-Reynolds number flow of two liquid films down an inclined plane. Phys Fluids A 5(12):3038–3048
22. Dyson RJ (2007) Mathematical modelling of curtain coating. D.Phil. thesis, University of Oxford
23. Goren S, Wronski S (1966) The shape of low-speed capillary jets of Newtonian liquids. J Fluid Mech 25(1):185–198
24. Tillett J (1968) On the laminar flow in a free jet of liquid at high Reynolds number. J Fluid Mech 32:273–292
25. Trouton F (1906) On the coefficient of viscous traction and its relation to that of viscosity. Proc R Soc 77:426–440